Short-Range Lurch Control In-Plane Switching Mode with Negative Dielectric Anisotropy Liquid Crystals

Toshiharu Matsushima, Shunichi Kimura, Shinichi Komura, Yuji Maede
Japan Display Inc., Chiba, Japan

Abstract
Shortening the response time of liquid crystals is crucial for improving the motion characteristic of liquid crystal display (LCD) technology. We report on short-range lurch control in-plane switching using negative dielectric anisotropy liquid crystals, which exhibit faster response times than positive ones. Our findings suggest flow during reorientation, offering insights for future LCD improvements.

Author Keywords
Fast response; fast switching; virtual reality; head-mounted display; in-plane switching; liquid crystal display; flow effect; negative dielectric anisotropy.

1. Introduction
In the modern digitized world, the role of electronic information displays has become increasingly important. In applications for rapidly advancing virtual reality (VR)/augmented reality (AR), improvements in characteristics such as high definition and high motion are desirable, and various display technologies such as organic light emitting diodes (OLED), micro light-emitting diodes (micro-LED), and liquid crystal display (LCD) are keeping pace in their development [1-3].

Shortening the response time of liquid crystals is an important element in improving the motion characteristics of LCD technology. For LCDs that are used in VR/AR applications, shortening the liquid crystal response time is a critical factor. The time required for one frame must be allocated between the circuit drive time, the lighting time, and the liquid crystal response time [3]. This also means that the demand for shorter response times becomes more stringent as the display achieves higher definition or uses a higher refresh rate. Therefore, response time has been an important research topic in recent years [4,5].

We previously reported on short-range lurch control in-plane switching (SLC-IPS) as an LCD mode that has a short response time [6-8]. SLC-IPS is achieved by controlling the planar orientation of the liquid crystals using the same materials and layer structure as the conventional IPS, thus shortening the response time of the LCDs. The response time matches well with Equation 1 predicted from continuum theory [8].

$$\tau_{decay-SLC} = \gamma_1 \Big/ \left[\frac{K_{22}}{d^2} + \frac{K_{11}}{\ell^2}\right]\pi^2 \qquad (1)$$

Here, τ is the response time, γ_1 is the rotational viscosity, K_{22} is the twist elastic constant, K_{11} is the splay elastic constant, d is the thickness of the liquid crystal layer, and ℓ is the lateral distance between the two non-responsive regions of the liquid crystal layer under the external electric field.

The SLC-IPS we have reported so far uses positive dielectric anisotropy liquid crystals (pSLC). Here, we report different characteristics for SLC-IPS that uses negative dielectric anisotropy liquid crystals (nSLC) from that using pSLC.

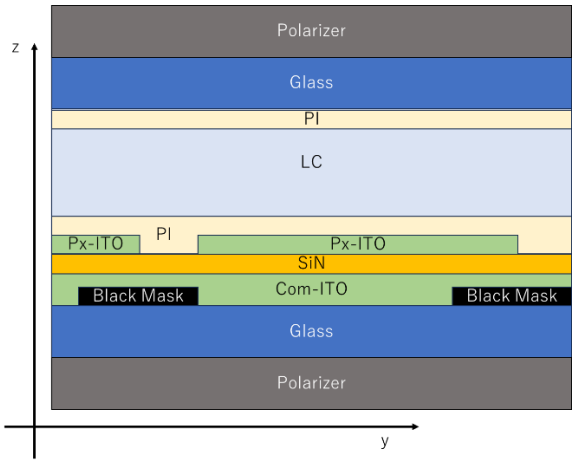

Figure 1. Cross-sectional structure of the test device.

2. Experiment
Test device: We fabricated a test device to evaluate nSLC. The cross-sectional structure of the test device is shown in Figure 1. On the glass substrate, indium tin oxide (ITO), silicon nitride (SiN), ITO, and polyimide alignment film (PI) are formed in this order, and the substrate with PI formed on the glass substrate becomes laminated. There is a liquid crystal layer in between the glass substrates. Black masks (BMs) are placed between the glass substrate and the ITO to shield the parts that do not contribute to the display. The polarizing plates are linear polarizing plates, and they are orthogonal to each other. To distinguish them, the ITO on the side of the glass substrate is called Com-ITO, and the ITO closer to the liquid crystal is called Px-ITO. The thickness of each layer is as follows: both ITO layers are 77 nm; the SiN layer is 200 nm; the liquid crystal layer is 2.5 µm.

The planar structure of the test device's electrode is shown in Figure 2. The unpatterned Com-ITO, SiN, and PI are omitted. We use a one-sided branch electrode structure [7], where the branch electrodes extend in the y-direction from the trunk electrode, which is oriented in the x-direction. The BM is positioned to hide the gaps between the ITO trunk electrodes and the branches. The branch electrodes of Px-ITO have a width L and a spacing S. Basically, they are fabricated with L = 1.9 µm, and S = 3.1 µm. The distance ℓ is estimated to be (L + S)/2 = 2.5 µm, since it is the distance between the non-rotating parts (i.e., imaginary boundaries) of the liquid crystal layer. As shown in Equation 1, ℓ is directly related to the response time of the SLC-IPS and. The length of the branch electrodes is 4.5 µm, forming a rectangular shape. We evaluated the change in transmittance when the diffused backlight was irradiated from the back by applying a voltage between the Px-ITO and Com-ITO to change the orientation of the liquid crystal.

ISSN 0097-996X/25/5603-2120-$1.00 © 2025

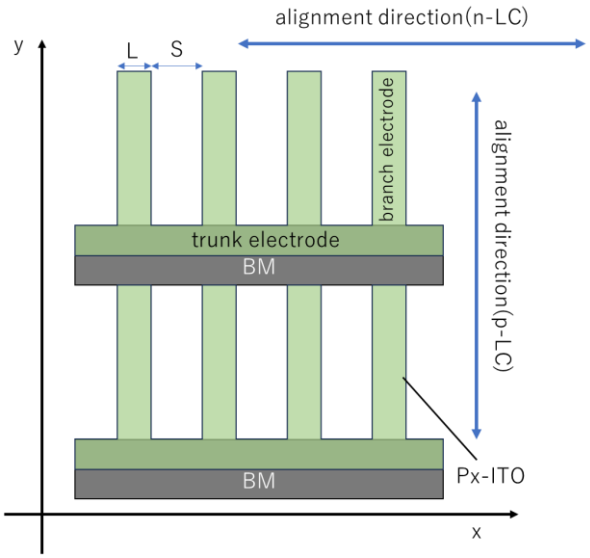

Figure 2. Planar structure of Px-ITO and BM.

3. Results and Discussion

Electro-optic characteristics:

The electro-optical characteristics of the pSLC and nSLC are shown in Figure 3. The anisotropy of the refractive index (Δn) of each type of liquid crystal is the same. The transmittance is defined as 1.0 when the polarizing plates are arranged in parallel.

In pSLCs, applying a high voltage changes the orientation direction of the liquid crystal molecules in an undesired direction. These disturbances in orientation produce areas of abnormal light transmission. This is a phenomenon that causes the distance between imaginary boundaries to widen in parts, which increases the transmittance but decreases the response time [7]. This occurs at approximately 7 V or more. In the case of nSLC, this problem does not occur due to changes in orientation caused by the application of high voltage.

Figure 4 shows microscopic images of pSLC and nSLC using different liquid crystals when a high voltage is applied. The orientation problem observed in pSLC is not observed in nSLC.

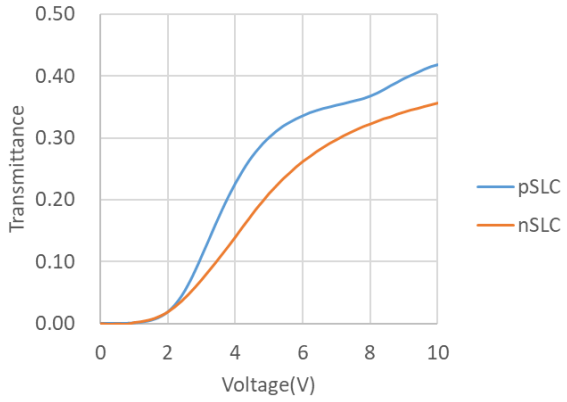

Figure 3. Electro-optic characteristics of the test device.

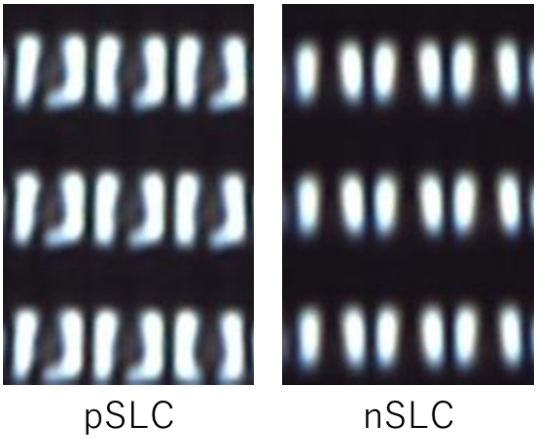

Figure 4. Microscopic images of pSLC and nSLC.

Whereas measures such as devising electrode structures are needed to solve this problem in pSLC, nSLC do not require such measures. This alleviation of restrictions on the electrode structure is advantageous when the pixel pitch becomes narrower.

Response time: The response time of nSLC was predicted from the continuum theory as Equation 2, similar to pSLC.

$$\tau_{decay-nSLC} = \gamma_1 \Big/ \left[\frac{K_{22}}{\boldsymbol{d}^2} + \frac{K_{33}}{\boldsymbol{\ell}^2}\right]\pi^2 \qquad (2)$$

where K_{33} is the bend elastic constant. The difference between this choice of elastic constant and Equation 1 is due to the difference in the initial alignment state.

The response time was calculated using the change in the transmittance when the voltage was changed from the applied state to the nonapplied state. The applied voltage was set to the value of the voltage just before the orientation problem occurred for pSLC, and it was set to 7.4 V for nSLC.

The measured results are shown in Figure 5. These results were obtained by measuring the response time of various liquid crystal materials having different characteristics in devices manufactured according to the same design.

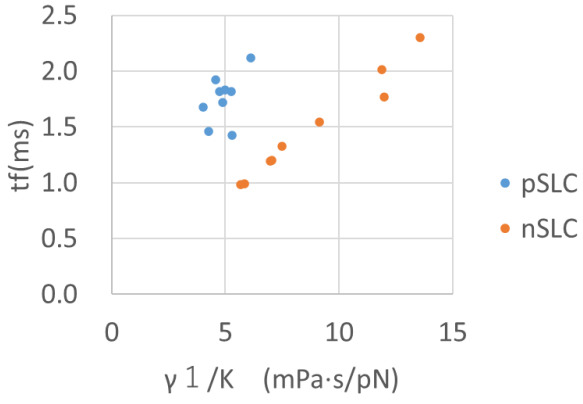

Figure 5. Comparison of the response times between pSLC and nSLC.

The time when the relative transmittance changes from 90% to 10% is defined as tf; the horizontal axis is γ_1/K_{11} for pSLC and γ_1/K_{33} for nSLC. Because we cannot directly compare the viscosity constants of pSLC and nSLC, we normalize them here using the elastic constant. These are related to the term distance ℓ that appears in Equations 1 and 2.

As can be seen from Figure 5, if the liquid crystals have the same viscosity constant divided by the elastic constant, the response time of nSLC will be shorter than that of pSLC. It is reasonable that there is variability in the tf of pSLC using liquid crystal materials with the same γ_1/ K_{11}, considering the influence of the γ_1/K_{22} term in Equation 1. In contrast, for the nSLC there is a very strong correlation between the response time and the value of γ_1/K_{33}.

To understand this point, we consider Equation 3, which is a transformation of Equation 2.

$$\frac{1}{\tau} = \frac{\pi^2 K_{33}}{\gamma_1 \ell^2} + \frac{\pi^2 K_{22}}{\gamma_1 d^2} \tag{3}$$

To consider the first term of Equation 3, we add the evaluation results for different distances ℓ. Therefore, we fabricated a test device for nSLC with L + S = 4 μm and carried out the same measurement. By adding the result of this measurement, we plot the reciprocal of the response time on the vertical axis and plot $\pi^2 K_{33}/\gamma_1 \ell^2$ on the horizontal axis in Figure 6.

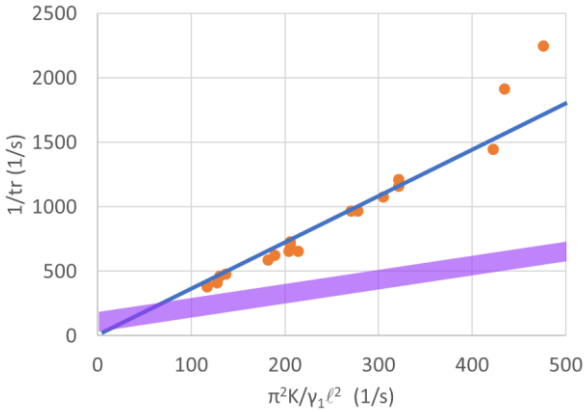

Figure 6. Analysis of the response time of the nSLC.

In Figure 6, a blue line is a line drawn appropriately along the entire plot with an intercept at 0. The range predicted from Equation 3 is indicated by the thick purple line.

A blue line with an intercept of 0 means that second term including d in Equation 3 is 0. This suggests that the response time of nSLC may have no dependence on the thickness of the LC layer. Additionally, the slope of the blue line is approximately 3.7, which deviates greatly from the prediction given by Equation 3. In the derivation of Equation 3, the viscosity coefficient that is related to the movement of the center of gravity is ignored. Therefore, we consider whether the center of gravity of the nSLC can move.

The simulation results for the alignment direction when the voltage is applied are compared side by side with the Px-ITO shape of the test device; they are shown in Figure 7.

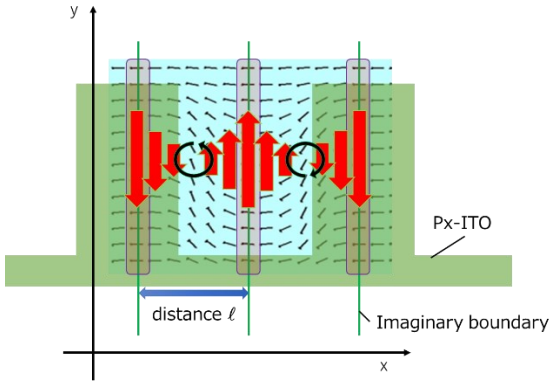

Figure 7. Alignment of the liquid crystal in the nSLC under the applied voltage, and the direction of torque on the liquid crystal when the voltage is turned off.

The green pattern is part of the Px-ITO. The black line is the alignment near the center of the liquid crystal layer when the voltage is applied. The green line along the y-axis is the imaginary boundary of the nSLC, the part where the liquid crystal does not rotate due to the application of voltage. The distance between the green lines is the distance ℓ in Equations 1, 2, and 3. When the voltage between Px-ITO and Com-ITO changes from this state to a non-voltage applied state, the liquid crystal alignment represented by the black line tends to return to the initial alignment parallel to the x-axis. At this time, the liquid crystals at the imaginary boundary do not rotate, and the liquid crystals between the imaginary boundaries rotate as shown by the circular arrow. As a result of this rotation, a flow occurs whose direction and size are indicated by the red arrow. In the x-direction, a gradient of the movement speed of the center of gravity of the liquid crystals occurs in the direction of distance ℓ. Because the liquid crystal at the imaginary boundary is not physically fixed, flow can occur in the liquid crystal molecules. We consider that this flow shown in Figure 7 causes to deviate from the results predicted by Equation 3.

4. Conclusion

Based on our findings, we conclude that the nSLC mode offers a significant advantage in terms of response time relative to the pSLC mode when the liquid crystals have the same viscosity constant divided by the elastic constant. This is primarily attributed to the difference in the initial alignment states.

Moreover, unlike pSLC, nSLC does not exhibit problems in orientation when a high voltage is applied, which eliminates the need for countermeasures such as devising electrode structures. Removing such restrictions on the electrode structure proves advantageous when the pixel pitch becomes narrower.

Our evaluation also suggests that the response time of the nSLC may not depend on the cell gap, and the flow caused by the movement of the center of gravity in the nSLC may be the cause of the deviation from the theoretical prediction. These findings provide valuable insights for future research and potential improvements in LCD technology.

5. References

1. Hsiang EL, Yang Z, Yang Q, Lan YF, Wu ST. Prospects and challenges of mini-LED, OLED, and micro-LED displays. J Soc Inf Disp. 2021;29(6):446-65. doi: 10.1002/jsid.1058.
2. Rao L, Argaman N, Zhuang J, Ninan A, Kim C, Wang D, et al. Display and optics architecture for meta's AR/VR development. IEEE Open J Immersive Disp. 2024. doi: 10.1109/OJID.2024.3370888.
3. Kim C, Klement A, Park E, Han J, Rao L, Zhuang J. 6-2: invited paper: high-PPI fast-switch display development for oculus Quest 2 VR headsets. SID Symp Dig Tech Pap. 2022;53(1):40-3. doi: 10.1002/sdtp.15410.
4. Cho AT, Du G, He Z, Wei C, Hsu J, Chen W. 31-4: curved and fast response time vertical-alignment (VA) liquid crystal gaming display development. SID Symp Dig Tech Pap. 2024;55(1):406-8. doi: 10.1002/sdtp.17543.
5. Chen SR, Choi WK. P-264: fast-response FFS LC device with multi-rubbing angle for VR applications. SID Symp Dig Tech Pap. 2024;55(1):2075-7. doi: 10.1002/sdtp.18011.
6. Matsushima T, Okazaki K, Yang Y, Takizawa K. 43.2: new fast response time in-plane switching liquid crystal mode. SID Symp Dig Tech Pap. 2015;46(1):648-51. doi: 10.1002/sdtp.10237.
7. Matsushima T, Kimura S, Komura S. Fast response in-plane switching liquid crystal display mode optimized for high-resolution virtual-reality head-mounted display. J Soc Inf Disp. 2021;29(4):221-9. doi: 10.1002/jsid.980.
8. Matsushima T, Seki K, Kimura S, Iwakabe Y, Yata T, Watanabe Y, et al. New fast response in-plane switching liquid crystal mode. J Soc Inf Disp. 2018;26(10):602-9. doi: 10.1002/jsid.708.